Journal of Power Sources 203 (2012) 153–158

Contents lists available at SciVerse ScienceDirect

Journal of Power Sources

journal homepage: www.elsevier.com/locate/jpowsour

An optimal strategy of electrolyte flow rate for vanadium redox flow battery

Xiangkun Ma[a], Huamin Zhang[a,*], Chenxi Sun[b], Yi Zou[b], Tao Zhang[b]

[a] R&D center for energy storage, Dalian Institute of Chemical Physics, Chinese Academy of Sciences, Dalian 116023, China
[b] Dalian RONGKEPOWER Co., Ltd., Dalian 116025, China

ARTICLE INFO

Article history:
Received 30 August 2011
Received in revised form 3 November 2011
Accepted 15 November 2011
Available online 25 November 2011

Keywords:
Vanadium redox flow battery
Electrolyte flow rate
Pump consumption
System efficiency

ABSTRACT

Electrolyte flow rate is a key factor that affects the performance of vanadium redox flow battery (VRFB). A kilo-watt class VRFB system is fabricated to investigate the effects of electrolyte flow rate on the performance of VRFB. The experiments show that the capacity increases, but the system efficiency decreases with the increase of electrolyte flow rate. An optimal strategy of electrolyte flow rate is proposed to improve the system efficiency and keep the high capacity simultaneously, which is corresponding to optimize the electrolyte flow rate at different stages of charge and discharge processes. The results show that the system efficiency can be improved as high as 8% when keeping high capacity simultaneously.

1. Introduction

The large scale energy storage technology becomes central topic of our times due to the request of grid load-leveling and smoothing output from renewable energy technologies. Vanadium redox flow battery (VRFB) is deemed to be one of the most suitable large-scale energy storage technologies due to its attractive features like flexible design, quick response, long cycle life and active thermal management [1].

Not like traditional batteries, the energy rating and power rating of VRFB are independent. The energy rating of a VRFB system is dependent on the concentration and the volume of the electrolyte, while the number of the cell stacks will determine the power rating of VRFB. The VRFB system consists of two electrolyte tanks filled with the electrolytes of V(II)/V(III) and V(IV)/V(V) in sulfuric acid solution, respectively, two electric pumps, and several cell stacks. The electrolytes were pumped into the cell stacks where electrochemical reaction occurred. The electric energy is stored and released by changing the valance of vanadium ions [2]. The higher electrolyte flow rate will increase the VRFB performance, especially for the capacity. But on the other hand the higher electrolyte flow rate will result in the larger pump consumption, which will reduce the system efficiency. Higher system efficiency is in contradiction with larger capacity. Therefore, the optimal electrolyte flow rate needs to be determined to balance the system efficiency and capacity. Up to now, most researches are focused on the key materials, such as electrode, electrolyte and ion exchange membranes [3–10]. There are rarely literatures reported on the optimization of the operation of VRFB.

In this paper, a kilo-watt class VRFB system is fabricated to investigate the effects of electrolyte flow rate on the performance of VRFB at different current densities. The strategies of electrolyte flow rate are optimized during charge process and discharge processes separately to improve the system efficiency and keep high capacity simultaneously. Finally, an optimal strategy of electrolyte flow rate for the charge–discharge cycle is presented and validated by experiments.

2. Experimental

2.1. VRFB system

A kilo-watt class VRFB system was fabricated to investigate the effects of electrolyte flow rate on the performance of VRFB. The VRFB system contained a kilowatt class module, two pumps, two electrolyte tanks, two flow meters, two heat exchangers and several pipes connecting all the equipments. The cell stack was manufactured by filter-pressing 15 VRFB single cells. The effective area of each electrode was 875 cm^2. Each single cell was fabricated with carbon felt, ion exchange membranes, carbon composited bipolar plates, PVC frames and gaskets. The volume of the electrolyte in each tank was 20 L containing 1.5 mol L^{-1} VO^{2+} in positive electrolyte and 1.5 mol L^{-1} V^{3+} in negative electrolyte, respectively. Two heat exchangers were used to control the electrolyte temperature in the range of 30–35 °C, and two differential flowmeters (RXDC-WAY25CEZX) were used to measure electrolyte flow rate. A

* Corresponding author. Tel.: +86 411 84379092; fax: +86 411 84665057.
E-mail address: zhanghm@dicp.ac.cn (H. Zhang).

0378-7753/$ – see front matter
doi:10.1016/j.jpowsour.2011.11.036

Table 1
Specification for VRFB system.

Specification Description	
Area of felt electrode	875 cm^2
Number of cells	15
Membrane material	Nafion 115 (Du Pont)
Material of electrode frame	PVC (polyvinyl chloride)
Material of end plate	Aluminum alloy
Electrolyte volume per half cell	20 L
Operating temperature	30–35 °C

power meter was used to measure power consumption of pumps at different flow rates. Table 1 listed the specifications of the VRFB system used in this experiment.

2.2. Charge–discharge performance

The charge–discharge performances of the VRFB system were conducted by using a battery testing system (Arbin Instruments Corp., USA). The upper limit voltage of charge was 23.25 V and the lower limit voltage of discharge was 15 V. The voltage, current, capacity (Ah) and energy (Wh) were recorded automatically by the battery testing system.

The charge–discharge performances at different current densities (45 mA cm^{-2} and 75 mA cm^{-2}) were tested at different electrolyte flow rates (from 0.20 $m^3 h^{-1}$ to 0.71 $m^3 h^{-1}$). The coulomb efficiency, voltage efficiency and energy efficiency were calculated according to formula (1)–(3). The pump consumption was measured by the power meter. And the system efficiency was calculated according to formula (4).

$$\text{Coulomb efficiency} = \frac{\text{Discharge capacity(Ah)}}{\text{Charge capacity(Ah)}} \times 100\% \quad (1)$$

$$\text{Voltage efficiency} = \frac{\text{Average discharge voltage(V)}}{\text{Average charge voltage(V)}} \times 100\% \quad (2)$$

$$\text{Energy efficiency} = \frac{\text{Discharge energy(Wh)}}{\text{Charge energy(Wh)}} \times 100\% \quad (3)$$

$$\text{System efficiency} = \frac{\text{Discharge energy(Wh)} - \text{Pump consumption(Wh) in Discharge}}{\text{Charge energy(Wh)} + \text{Pump consumption(Wh) in Charge}} \times 100\% \quad (4)$$

The similar charge–discharge cycles were conducted in the experiments in order to ensure the accuracy of the research. Firstly, the VRFB system was tested at flow rate of 0.20 $m^3 h^{-1}$ and then increased flow rate to 0.71 $m^3 h^{-1}$ when charged the VRFB to 23.1 V, 22.95 V, 22.8 V, 22.65 V and 22.5 V, respectively during the charge process, while at flow rate of 0.71 $m^3 h^{-1}$ during discharge process. Secondly, the VRFB system was tested at flow rate of 0.71 $m^3 h^{-1}$ during charge process, while at flow rate of 0.20 $m^3 h^{-1}$ and then increased flow rate to 0.71 $m^3 h^{-1}$ when discharged to 15.6 V, 16.2 V, 16.8 V, 17.4 V and 18 V, respectively during discharge process. Finally, the VRFB system was tested with an optimal strategy of electrolyte flow rate for the charge–discharge cycle.

3. Results and discussion

3.1. Effects of electrolyte flow rate on the performance of VRFB

The VRFB system is tested at current densities of 45 mA cm^{-2} and 75 mA cm^{-2} when operating at different flow rates. Flow rates of 0.20 $m^3 h^{-1}$, 0.30 $m^3 h^{-1}$, 0.40 $m^3 h^{-1}$, 0.51 $m^3 h^{-1}$, 0.61 $m^3 h^{-1}$ and 0.71 $m^3 h^{-1}$ are chosen as the operating flow rate. The coulomb efficiency, voltage efficiency and energy efficiency of the VRFB system are shown in Fig. 1. When operating at 45 mA cm^{-2}, it can be seen that coulomb efficiency decreases slowly from 92.1% to 91.6%, while voltage efficiency increases by 3.77% with the increase of flow rate from 0.20 $m^3 h^{-1}$ to 0.71 $m^3 h^{-1}$. And energy efficiency increases from 78.4% to 81.38%. The similar trend is presented when operating at 75 mA cm^{-2}. It shows that coulomb efficiency takes on a small decrease from 94.4% to 93.8%, while voltage efficiency increases by 5.6% when increasing flow rate from 0.20 $m^3 h^{-1}$ to 0.71 $m^3 h^{-1}$. And energy efficiency increases from 75.03% to 77.97%.

Fig. 2 shows the charge–discharge curves when operating at 45 mA cm^{-2} and 75 mA cm^{-2}. The capacity of VRFB system is much higher at the operating condition of 45 mA cm^{-2} than that operates at 75 mA cm^{-2} at the same flow rate. For example, when operating at 45 mA cm^{-2}, the capacity increases from 29 Ah to 35.5 Ah with increase of flow rate from 0.2 $m^3 h^{-1}$ to 0.71 $m^3 h^{-1}$, while the capacity increases from 14.3 Ah to 24.5 Ah when operating at 75 mA cm^{-2}.

Fig. 3 shows the open circuit voltage (OCV) after charge and discharge when operating at 45 mA cm^{-2} and 75 mA cm^{-2}. The OCV increases after charge and decreases after discharge with the increase of flow rate respectively. It is well known that the OCV is related to state of electrolyte. At the same operating current density, more capacity will be obtained with higher OCV after charge and lower OCV after discharge. It means that the capacity will increase with increase of flow rate, which is consistent with the phenomenon presented in Fig. 2.

In practical operation of VRFB, system efficiency is more significant than energy efficiency because of pump consumption. Fig. 4 shows the energy efficiency, system efficiency and capacity of VRFB at current density of 45 mA cm^{-2} and 75 mA cm^{-2} when operating at different flow rates. It can be seen that the energy efficiency and capacity increase, but the system efficiency decreases with increase of flow rate. For example, when operating at 75 mA cm^{-2}, the energy efficiency increases from 72.9% to 78%, but the system

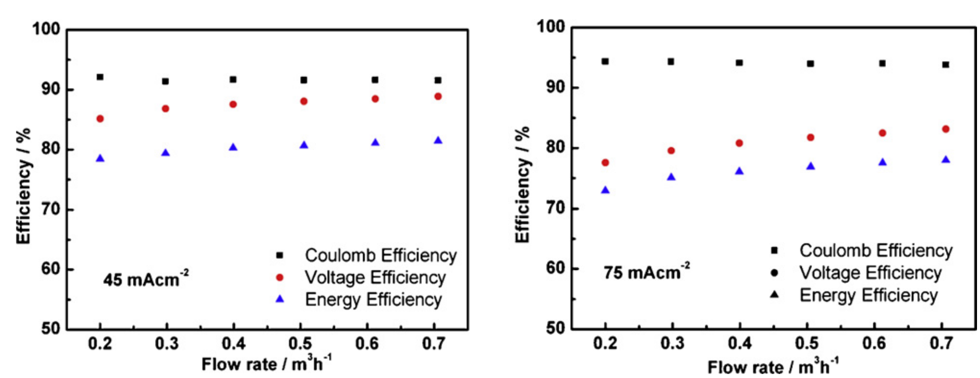

Fig. 1. Efficiencies of VRFB at current density of 45 mA cm^{-2} and 75 mA cm^{-2} when operating at different flow rates.

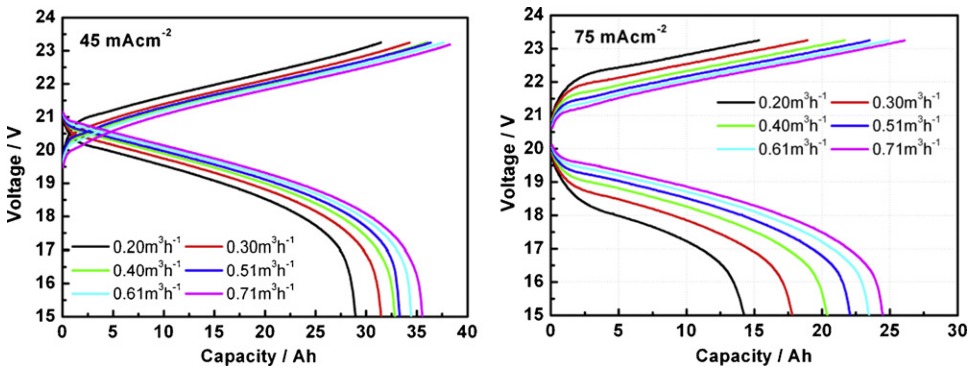

Fig. 2. Charge–discharge curves at current density of 45 mA cm^{-2} and 75 mA cm^{-2} when operating at different flow rates.

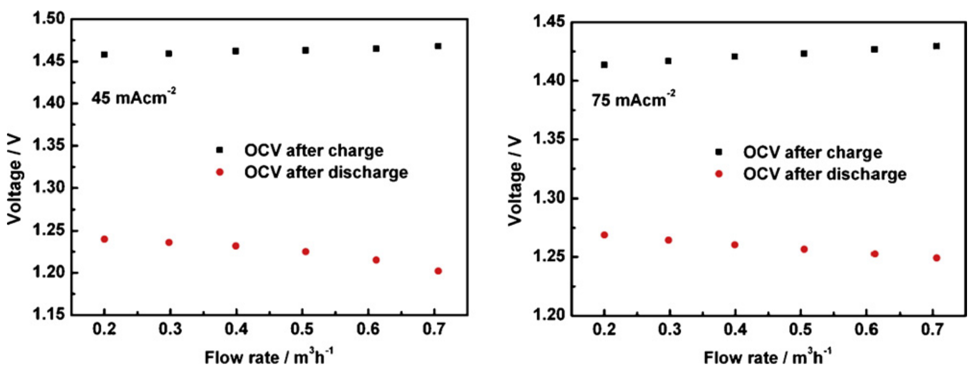

Fig. 3. OCVs after charge process and discharge process at current density of 45 mA cm^{-2} and 75 mA cm^{-2} when operating at different flow rates.

efficiency decreases from 69.3% to 58.5% with increase of flow rate from 0.2 m^3 h^{-1} to 0.71 m^3 h^{-1}. The capacity increases from 14.3 Ah to 24.5 Ah. The results show that the system efficiency and capacity have the opposite trend with the increase of flow rate.

It can be found that all the performance, including energy efficiency, system efficiency and capacity, have nearly the same trend with the increase of flow rate when operating at different current densities. However, different flow rates are needed to keep the same system efficiency and capacity when operating at different current densities. For example, flow rates of 0.4 m^3 h^{-1} and 0.5 m^3 h^{-1} are needed to obtain a system efficiency of 65% when operating at 45 mA cm^{-2} and 75 mA cm^{-2}, respectively.

3.2. Strategy of electrolyte flow rate for charge process

System efficiency and capacity play significant roles in an operating VRFB system. High system efficiency and capacity are preferred to reduce capital cost and operating cost in practical application. As discussed above, capacity will increase with the increase of flow rate, while system efficiency shows opposite trend to flow rate. The reason is that the increase of flow rate will reduce concentration polarization, and further increase capacity. However, the higher pump consumption will reduce system efficiency as well. It is well known that the requirement of electrolyte flow rate increases at the end of charge (and discharge) process because the vanadium ions V^{3+} and V^{4+} (and V^{2+} and V^{5+}) decrease sharply. On the other hand the requirement of electrolyte flow rate is relatively lower in the initial of charge (and discharge) process because the vanadium ions V^{3+} and V^{4+} (and V^{2+} and V^{5+}) are much more sufficient. Electrolyte flow rate should be optimized during charge–discharge process. In this paper, some strategies of electrolyte flow rate are put forward to increase system efficiency as far as possible and keep high capacity with that operates at Q_{high}. Considering the similar trend at different current densities, 75 mA cm^{-2} is chosen for the next experiments.

In order to improve system efficiency and keep high capacity simultaneously, the VRFB system operates at Q_{low} (0.20 m^3 h^{-1}) and then increases flow rate to Q_{high} (0.71 m^3 h^{-1}) at the end of charge process, while the flow rate always is kept high (0.71 m^3 h^{-1}) in discharge process. The voltage of 23.1 V, 22.95 V, 22.8 V, 22.65 V

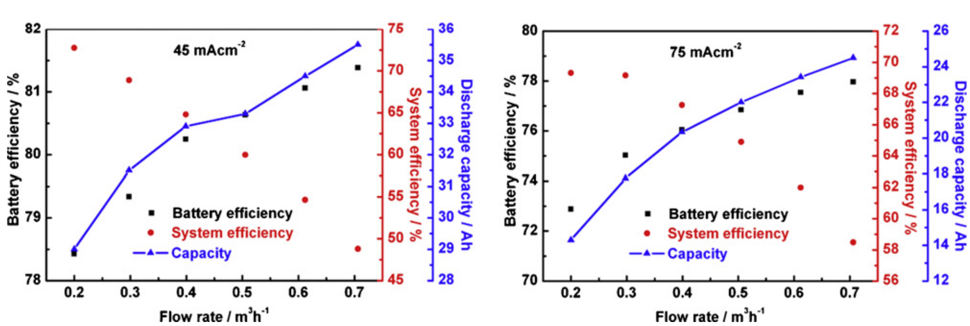

Fig. 4. Energy efficiency, system efficiency and capacity at current density of 45 mA cm^{-2} and 75 mA cm^{-2} when operating at different flow rates.

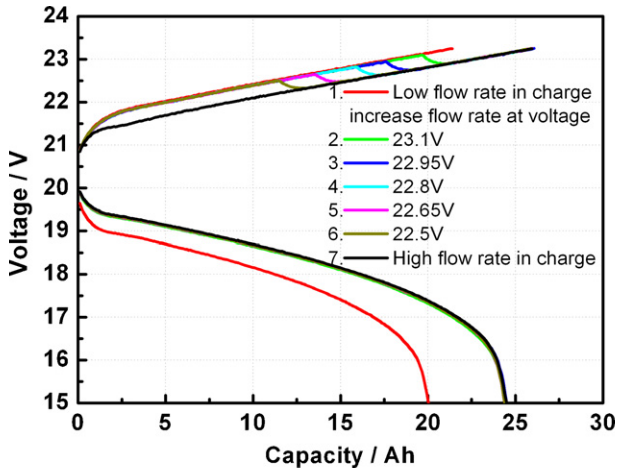

Fig. 5. Charge–discharge curves at different operating modes when using an optimal strategy of flow rate for charge process.

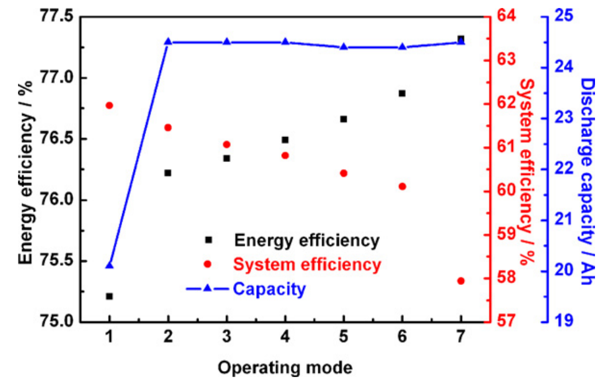

Fig. 7. Energy efficiency, system efficiency and capacity at different operating modes when using an optimal strategy of flow rate for charge process.

and 22.5 V are chosen as the points that increase flow rate, corresponding to several operating modes listed in Fig. 5. It can be seen that the charge curves after increasing flow rate are all overlap the curves that always operates at Q_{high}. The discharge curves are all overlap except for operating at Q_{low} during charge process. It is well known that the concentration polarization can be decreased with the increase of flow rate, which will lead to the reduction of charge voltage. In this experiment, when increasing flow rate from 0.20 $m^3\,h^{-1}$ to 0.71 $m^3\,h^{-1}$, the concentration polarization reduces gradually to the level that operates at Q_{high}. It also means the same capacity can be obtained by using this strategy that increases flow rate from 0.20 $m^3\,h^{-1}$ to 0.71 $m^3\,h^{-1}$ at the end of charge process.

The OCV after charge and discharge are shown in Fig. 6. The index in *X*-axis is corresponding to operating mode listed in Fig. 5. Excluding operating mode 1, which operates at Q_{low} during charge, the others are all present the same OCV after charge or discharge process. It also means that the states of electrolyte after charge or discharge are all the same except for operating at mode 1. For operating mode 1, which operates at Q_{low} during charge process, the OCV after charge is lower than others because the concentration polarization is larger when operating at Q_{low}, which results in the increase of charge voltage. So the gap between OCV and cut-off voltage is larger. The OCV after discharge is the same as the others, because flow rate is the same during discharge process.

Fig. 7 shows the energy efficiency, system efficiency and capacity when operating at different modes. It can be figured out that the energy efficiency increases from 76.2% to 77.3% when operating mode changes from mode 2 to mode 7, while the system efficiency decreases from 61.5% to 58.0% simultaneously. Especially, the system efficiency decreases sharply by 2.2% when operating at mode 7. At the same time, the capacity almost keeps stable, which changes from 24.4 Ah to 24.5 Ah. Although operating mode 1 shows the highest system efficiency 62.0%, its capacity is only 20.1 Ah.

The comparison between these seven operating modes shows that the capacity is the same as that always operates at Q_{high} (mode 7), however its system efficiency increases by 3.5% when operating at mode 2. So the mode that operates at Q_{low} and then increases flow rate to Q_{high} at voltage of 23.1 V during charge process is the optimal strategy.

3.3. Strategy of electrolyte flow rate for discharge process

In Section 3.2, the strategy of flow rate during charge process is optimized. In this section, the similar experiments are carried out in order to optimize flow rate during discharge process. The VRFB system operates at Q_{low} and then increase flow rate to Q_{high} during discharge process, while the flow rate during charge process always is kept high (0.71 $m^3\,h^{-1}$). The voltage of 15.6 V, 16.2 V, 16.8 V, 17.4 V and 18 V are chosen as the points that increase flow rate, corresponding to several operating modes listed in Fig. 8. It can be figured out that the charge curves almost overlap the curve that always operates at Q_{high} after increasing the

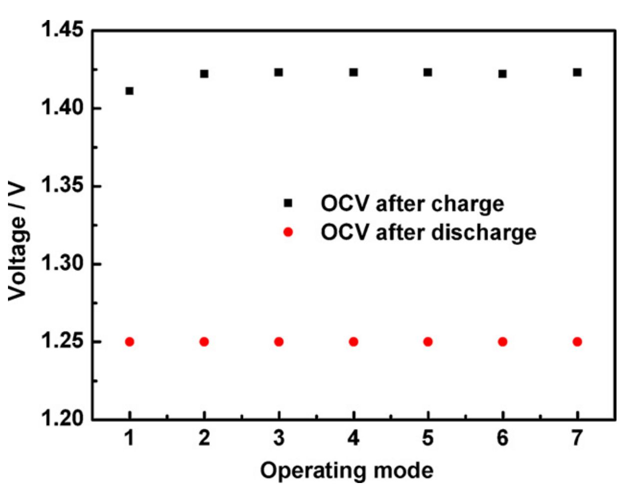

Fig. 6. OCVs after charge process and discharge process at different operating modes when using an optimal strategy of flow rate for charge process.

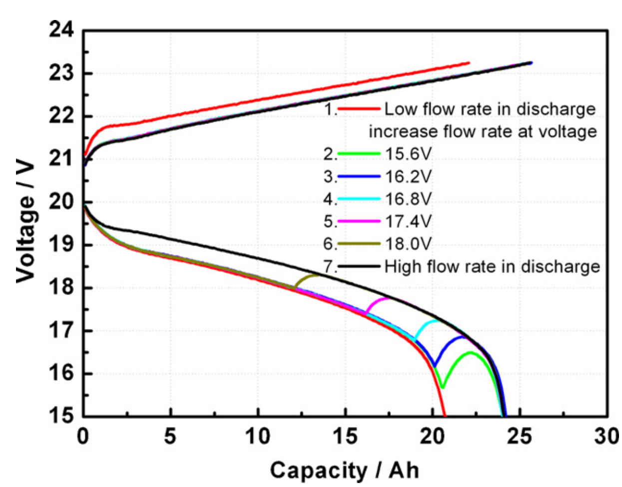

Fig. 8. Charge–discharge curves at different operating modes when using an optimal strategy of flow rate for discharge process.

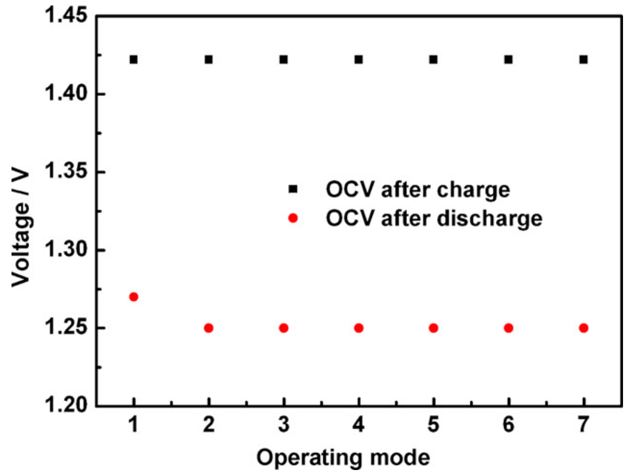

Fig. 9. OCVs after charge process and discharge process at different operating modes when using an optimal strategy of flow rate for discharge process.

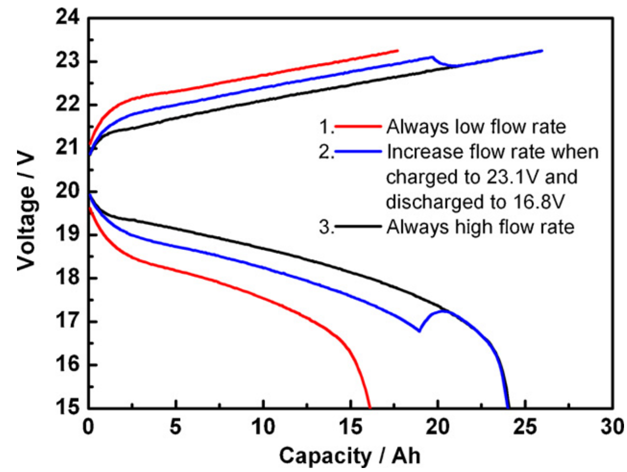

Fig. 11. Charge–discharge curves at different operating modes when using an optimal strategy of electrolyte flow rate for charge–discharge cycle.

flow rate during discharge process. The charge curves are all overlap except for operating at Q_{low} during discharge process. The same reason with discussed above is that the concentration polarization reduces with the increase of flow rate, which will also result in the increase of discharge voltage. In this experiment, when increasing flow rate from Q_{low} to Q_{high}, the concentration polarization reduces gradually to the level that operates at Q_{high}, so the discharge curve coincides with the curve that always operates at Q_{high}. It also means the same capacity can be obtained by using this strategy that increases flow rate to Q_{high} at the end of discharge process.

The OCV after charge and discharge are shown in Fig. 9. The index in *X*-axis is corresponding to operating mode listed in Fig. 8. Excluding operating mode 1, which operates at Q_{low} in discharge, the others are all present the same OCV after charge or discharge process. The reason is the same as that discussed in Section 3.2.

Fig. 10 shows the energy efficiency, system efficiency and capacity when operating at different modes. It can be figured out that the energy efficiency increases from 75.2% to 76.5% when operating mode changes from mode 2 to mode 7. The trend of system efficiency shows a little different with that in Section 3.2. The system efficiency increases gradually and then decreases sharply. The highest system efficiency 63.8% is obtained when operating at mode 4, which increases flow rate at voltage of 16.8 V. And at the same time, the capacity almost keeps stable, which changes from 24.2 Ah to 24.4 Ah. Although operating mode 1 shows the highest system efficiency 65.1%, its capacity is only 20.8 Ah, which is much lower than others.

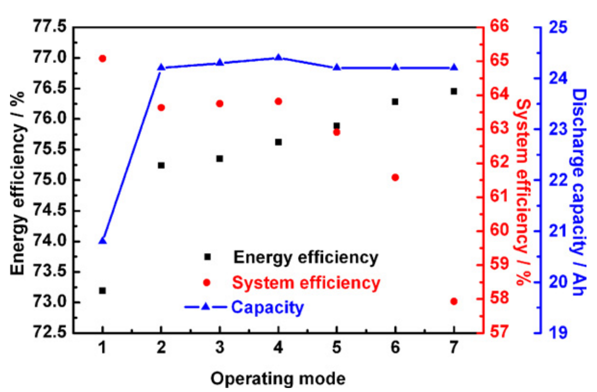

Fig. 10. Energy efficiency, system efficiency and capacity at different operating modes when using an optimal strategy of flow rate for discharge process.

The comparison between these seven operating modes shows that the capacity is nearly the same as that operates at Q_{high} (mode 7), but the system efficiency increases by 5.9% when operating at mode 4. So the mode that operates at Q_{low} and then increases flow rate to Q_{high} at voltage of 16.8 V during discharge process is the optimal strategy.

3.4. Strategy of electrolyte flow rate for charge–discharge cycle

The optimal strategies of flow rate during charge and discharge process are discussed respectively in sections above, and the optimal points of voltage at which increase flow rate to Q_{high} are determined. In this section, the optimal strategy of electrolyte flow rate for charge–discharge cycle is proposed, which is the combination of strategies for charge and discharge process. As described in Sections 3.2 and 3.3, the VRFB system operates at Q_{low} and then increases flow rate to Q_{high} at voltage of 23.1 V during charge process, while operates at Q_{low} and then increases flow rate to Q_{high} at voltage of 16.8 V during discharge process. The optimal strategy of electrolyte flow rate for charge–discharge cycle is applied to investigate its effect on the system efficiency and capacity.

The charge–discharge curve based on the optimal strategy is shown in Fig. 11. The charge–discharge curve overlaps the curve that always operates at Q_{high}. The reason is that the concentration polarization will be decreased by increasing flow rate, which will

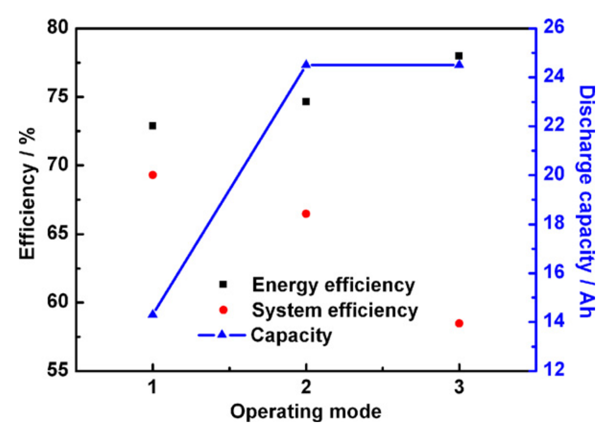

Fig. 12. Energy efficiency, system efficiency and capacity at different operating modes when using an optimal strategy of electrolyte flow rate for charge–discharge cycle.

Table 2
Comparison of the performance of different operating modes.

	Energy efficiency (%)	System efficiency (%)	Discharge capacity (Ah)
Always operating at Q_{low}	72.9	69.3	14.3
Optimal strategy used in charge process	76.2	61.5	24.5
Optimal strategy used in discharge process	75.6	63.8	24.4
Optimal strategy used in charge–discharge cycle	73.7	66.5	24.5
Always operating at Q_{high}	78.0	58.5	24.5

lead to the decrease of charge voltage and the increase of discharge voltage as shown in Fig. 11.

Fig. 12 lists the energy efficiency, system efficiency and capacity of three operating modes as described in Fig. 11. It can be found that the system efficiency of model 2 is much higher than that of model 3, while the capacity keeps unchanged. Although the system efficiency of model 2 is slightly lower than that of model 1, the capacity of model 2 is much higher than that of model 1.

Table 2 lists the energy efficiency, system efficiency and capacity when operating at different modes. It can be easily figured out that the highest capacity can be obtained when operating with any optimal strategies of flow rate. But the system efficiency shows a little different. The maximum increase of the system efficiency is obtained by using the optimal strategy of electrolyte flow rate for charge–discharge cycle, which is improved as high as 8%. The results show that the optimal strategy of electrolyte flow rate can increase system efficiency and keep high capacity at the same time.

Furthermore, the optimal strategy of flow rate for VRFB is obtained based on the experiment that operates at 75 mA cm^{-2}. If operating at different current densities, the optimal strategy of flow rate will be a little different, but the trend is certain to be similar.

4. Conclusions

The effects of electrolyte flow rate on the performance of VRFB are investigated by a kilo-watt class VRFB system. The results show that the capacity increase, but the system efficiency decreases with increase of electrolyte flow rate at a constant current density. In order to improve system efficiency and keep high capacity at the same time, an optimal strategy of electrolyte flow rate for charge–discharge cycle of VRFB is proposed. In charge process VRFB operates at the lower flow rate of 0.2 $m^3\,h^{-1}$, and then increases flow rate to 0.71 $m^3\,h^{-1}$ when the voltage increases to 23.1 V. In discharge process VRFB operates at the lower flow rate of 0.2 $m^3\,h^{-1}$, and then increases flow rate to 0.71 $m^3\,h^{-1}$ when the voltage decreases to 16.8 V. The system efficiency can be improved as high as 8% compared with that operating always at the high flow rate of 0.71 $m^3\,h^{-1}$. The results show that the optimal strategy of electrolyte flow rate is valid and helpful for the operation of VRFB.

Acknowledgement

Financial support from '973′ project of MOST (Ministry of Science and Technology of China) (2010CB227205) is gratefully acknowledged.

References

[1] M. Skyllas-Kazachos, et al. All-vanadium redox battery. United States Patent, No4786567, Nov. 1988.
[2] C.X. Sun, J. Chen, H.M. Zhang, X. Han, Q.T. Luo, J. Power Sources 195 (2010) 890–897.
[3] E. Wiedemann, A. Heintz, R.N. Lichtenthaler, J. Membr. Sci. 141 (1998) 207–213.
[4] T. Sukkar, M. Skyllas-Kazacos, J. Membr. Sci. 222 (2003) 235–247.
[5] T. Mohammadi, S.C. Chieng, M. Skyllas-Kazacos, J. Membr. Sci. 133 (1997) 151–159.
[6] M. Vijayakumar, S.D. Burton, C. Huang, L. Li, Z.G. Yang, G.L. Graff, J. Liu, J.Z. Hu, M. Skyllas-Kazachos, J. Power Sources 195 (2010) 7709–7717.
[7] H. Kaneko, K. Nozaki, Y. Wada, T. Aoki, A. Negishi, M. Kamimoto, Electrochim. Acta 36 (1991) 1191–1196.
[8] H.Q. Zhu, Y.M. Zhang, L. Yue, W.S. Li, G.L. Li, D. Shu, H.Y. Chen, J. Power Sources 184 (2008) 637–640.
[9] P. Qian, H.M. Zhang, J. Chen, Y.H. Wen, Q.T. Luo, Z.H. Liu, D.J. You, B.L. Yi, J. Power Sources 175 (2008) 613–620.
[10] M. Vijayakumar, L. Li, G. Graff, J. Liu, H.M. Zhang, Z.G. Yang, J.Z. Hu, J. Power Sources 196 (2011) 3369–3672.